Additive colouring of CaF_2:Yb crystals: determination of Yb^{2+} concentration in CaF_2:Yb crystals and ceramics

A. S. Shcheulin, A. E. Angervaks, T. S. Semenova, L. F. Koryakina, M. A. Petrova, P. P. Fedorov, V. M. Reiterov, E. A. Garibin, et al.

Applied Physics B
Lasers and Optics

ISSN 0946-2171
Volume 111
Number 4

Appl. Phys. B (2013) 111:551-557
DOI 10.1007/s00340-013-5372-y

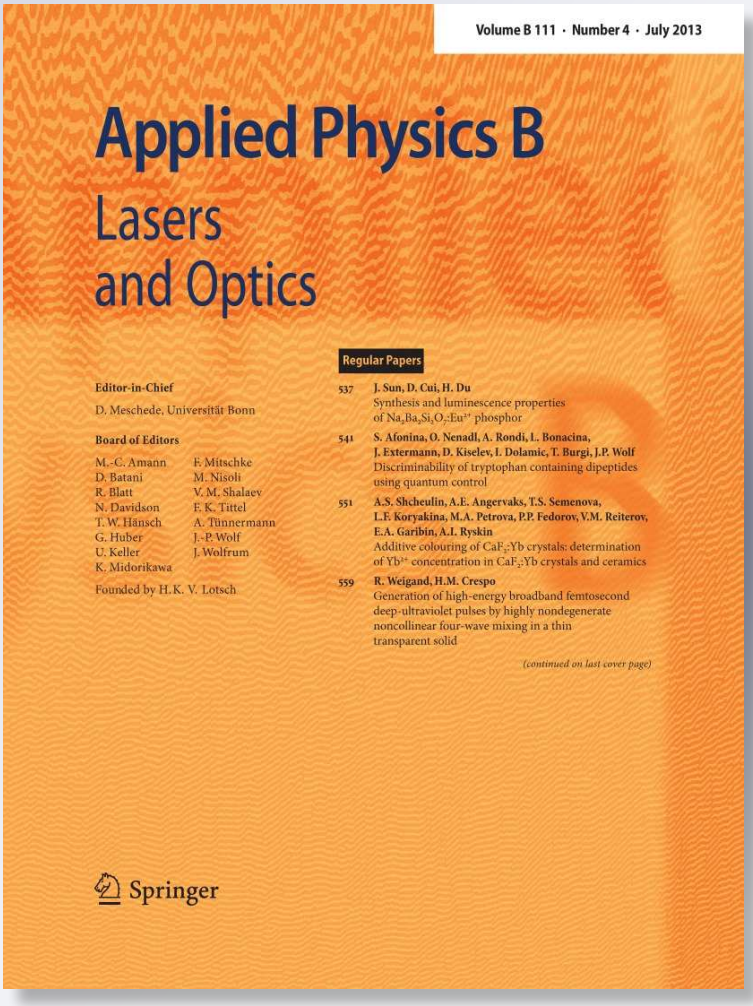

Springer

Appl. Phys. B (2013) 111:551–557
DOI 10.1007/s00340-013-5372-y

Applied Physics B
Lasers and Optics

Additive colouring of CaF_2:Yb crystals: determination of Yb^{2+} concentration in CaF_2:Yb crystals and ceramics

A. S. Shcheulin · A. E. Angervaks · T. S. Semenova · L. F. Koryakina · M. A. Petrova · P. P. Fedorov · V. M. Reiterov · E. A. Garibin · A. I. Ryskin

Received: 24 September 2012 / Accepted: 6 February 2013 / Published online: 10 March 2013

Abstract When growing CaF_2 crystal doped with rare-earth ions, most of these ions are present in a trivalent state. However, due to contact with graphite crucible, a small proportion of a number of ions (Eu, Sm, Yb and Tm) are reduced to a bivalent state. A similar situation takes place during fabrication of CaF_2 ceramics doped with rare-earth metals. This fact is of particular importance for laser CaF_2:Yb crystals (ceramics), a promising material for short-pulse, high-power, high-energy diode-pumped solid state lasers since the presence of bivalent Yb ions can be a source of thermal losses. To date, there has been no technique to determine Yb^{2+} concentration in as-grown crystals. The proposed technique is based on a total reduction of Yb^{3+} ions via the heating of as-grown CaF_2 crystals with known concentration of Yb in the reducing atmosphere of metal vapour and determining the cross section of absorption bands of Yb^{2+} ions. The knowledge of these parameters allows estimation of the Yb^{2+} content in CaF_2:Yb crystals or ceramics by analysing their absorption spectra. Examples of using this technique are given. The technology of CdF_2 crystals reduction (an "additive colouring") and features of colouring of crystals doped with rare-earth ions are considered.

A. S. Shcheulin · A. E. Angervaks (✉) ·
T. S. Semenova · L. F. Koryakina · M. A. Petrova · A. I. Ryskin
National Research University of Information Technologies, Mechanics and Optics, Kronverkskiy pr., 49, 197101 Saint Petersburg, Russia
e-mail: angervax@mail.ru

P. P. Fedorov
A.M. Prokhorov General Physics Institute, Vavilov str., 38, 119991 Moscow, Russia

V. M. Reiterov · E. A. Garibin
INCROM Ltd., Babushkina str., 36, bld. 1, 192171 Saint Petersburg, Russia

1 Introduction

The trivalent ytterbium ion, when compared with the widely used neodymium ion, has significant advantages as a dopant of diode-pumped lasers media [1]. Since the first laser studies of CaF_2:Yb crystals [2–4], this medium has attracted a growing interest for use in short-pulse, high-power, high-energy solid-state lasers [5–7]. This interest is determined by a variety of reasons, in particular its good thermal properties [8–11], very broad emission band, the absence of concentration quenching and the existing technology for the growth of high-quality crystals of large dimension.

Absorption and emission spectra of crystals with Yb content ranging from several tenths up to tens of percent do not change since, in this concentration range, rare-earth (RE) ions form predominantly hexamer Yb_6F_{37} clusters. These clusters are well embedded into the crystal lattice since they are actually identical in shape and dimensions to a structure Ca_6F_{32} unit of the lattice [12–17].

The detailed review of laser characteristics of CaF_2:Yb and SrF_2:Yb crystals is given in [18].

Despite numerous merits of CaF_2:Yb crystals, CaF_2:Yb ceramics can have a preference for greater laser damage resistance due to the absence of cleavage planes. Therefore, considerable efforts are being made to develop the CaF_2:Yb ceramics laser medium [19–21]; they are resulted in production of high-quality laser ceramics [22, 23].

The growth of CaF_2:Yb single crystals and fabrication of ceramics take place under weakly reducing conditions due to their contact with the equipment and vacuum.

Correspondingly, this growth/fabrication is accompanied with a partial $Yb^{3+} \rightarrow Yb^{2+}$ conversion [23–25]. Ultraviolet (UV) absorption bands of Yb^{2+} ions make non-radiative losses possible due to the many-photon absorption of the exciting radiation. These losses should grow with the growth of Yb concentration, N(Yb).

Establishing the influence of Yb^{2+} content on the efficiency of conversion of the pump energy into laser emission is hampered by the absence of techniques for determination of Yb^{2+} concentration, $N(Yb^{2+})$, in CaF_2 crystals/ceramics. In this article, such a technique is described.

The technique is based on the total reduction of Yb^{3+} ions in as-grown CaF_2 crystal with a known concentration of Yb and determination of a cross section of Yb^{2+} absorption bands. The knowledge of this parameter allows the determination of Yb^{2+} content by analysing absorption spectrum of as-grown CaF_2:Yb crystals or as-fabricated CaF_2:Yb ceramics.

One should note that in the natural species of CaF_2 crystals (fluorite mineral), which contain RE ions, some of them (Sm, Eu, Tm, Yb) are present in a bivalent state.

Attempts to reduce impurity RE ions in synthetic CaF_2 crystal have been initially made using ionizing γ-radiation [26]. It was found, however, that this technique does not allow the total reduction of the ions [27]. An electrolytic reduction was also used for this purpose [28]; this technique also does not permit total RE reduction. The most effective method is a thermo-chemical reduction of RE ions in CaF_2 crystals by heating in metal-cation vapours (an "additive colouring" of the crystals). Such a reduction was first described in [29] using a vacuum-treated ampoule containing the crystal and a piece of metal (Ca). This technique has been widely used in the study of bivalent RE ions in CaF_2 crystals.

The most effective technology for the additive colouring of CaF_2 crystals is considered in Sect. 2. In Sect. 3, the features of colouring of Yb-doped crystals are discussed. Parameters necessary for determination of Yb^{2+} concentration in CaF_2 crystals and ceramics are given in Sect. 4.

2 Additive colouring of CaF_2 crystals

In this article, the additive colouring of CaF_2 crystals was performed in a heat-pipe-type set-up, which allows almost independent management of the two important parameters of the process: pressure of the metal vapour and coloured crystal temperature, T [30, 31].[1] The separate management is provided with a buffer inert gas (helium) that determines the pressure in the system, p. The heat pipe is an evacuated stainless-steel cylinder with its lower part heated by a furnace to the temperature dependent on the colouring regime, whereas its upper part is maintained at room temperature by a refrigerator, the water cooled stainless steel tube encircled the middle part of the pipe (Fig. 1). The container with sample to be coloured is placed on the end of the metal rod (manipulator) that is pulled down into the lower part of the heat pipe. In the same part of the tube but outside the container, a metal piece is placed. The gradient of the metal vapour concentration in the gas phase results from displacement of lightweight helium by metal vapour to the upper part of the set-up to the level of the dew point. The metal is condensed at that level, flows down to the lower (hot) part of the pipe and evaporates. Thus, the separation of components in a "helium–metal vapour" in the vapour–gas mixture is of a dynamic nature. Under these conditions, the pressure in the system is controlled by the buffer gas (helium) and is barely dependent on the temperature of the crystal that is located in the hot zone.

The dynamic mode of the heat-pipe operation, which implies the continuous circulation of metal within the cylinder, is implemented at the fairly low pressure of metal vapour at its freezing temperature (the dew point). Otherwise, the metal would freeze out, i.e. would condense into the solid phase in the upper (cold) part of the pipe. Calcium does not meet this condition, whereas all the alkali metals do. Based on this reasoning, it is expedient to colour CaF_2 crystals in a lithium-calcium mixture. In this case, the dew point is determined by lithium, which is dominant in the

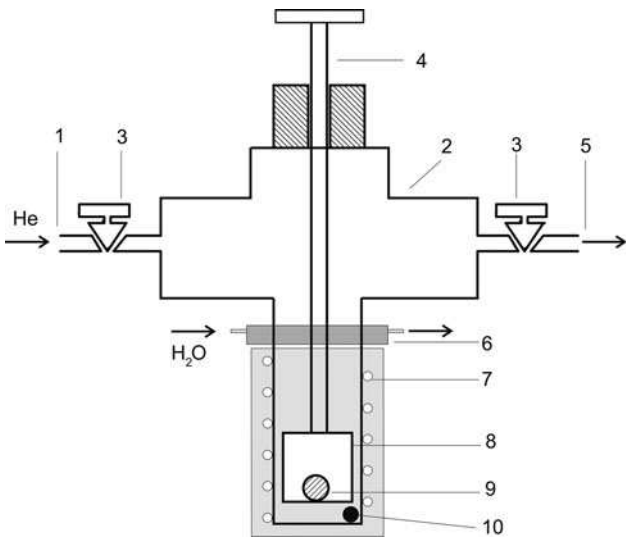

Fig. 1 Schematic of the heat-pipe system: *1* helium supply, *2* stainless steel vacuum chamber, *3* vacuum valve, *4* manipulator for displacing the container with a sample, *5* line to the vacuum pump, *6* water cooled refrigerator, *7* furnace, *8* container, *9* sample and *10* piece of metal

[1] Earlier, a similar type of set-up was used for additive colouring of alkali-halide crystals [32].

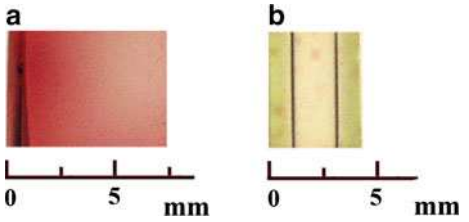

Fig. 2 Photographs of samples' cross-sections of **a** non-doped CaF_2 after 15 min of additive colouring, **b** CaF_2:Yb (Sample 2) after two 5 h cycles of colouring. The coloured segments of non-doped crystal are *reddish* due to the colour centre's absorption whereas these segments in Yb-doped crystal have a weakly greenish shade, probably determined by Ce centres, which are formed in additively coloured crystals (this proposal is confirmed by presence of Ce^{3+} band 306 nm in spectra of as-grown crystals, see Fig. 3) [33, 34]. The *dark lines* in (**b**) mark the planes, along which light propagation is impossible, probably due to a steep refractive index change

composition, whereas the colouring agent is calcium vapour. The composition was chosen to ensure melting at a temperature close to the lithium-melting temperature. This condition is satisfied when the calcium content in the lithium–calcium mixture does not exceed 2 at.%. In the metal composition used, this value was about 1 at.%.

One should note that due to the distinction in the metal masses, the heat-pipe regime can also be implemented for the metal vapour mixture by itself, which leads to its separation with increasing partial pressure of the calcium vapour. This separation is insignificant at high pressure of vapour-gas mixture because of the small content of calcium atoms in the mixture. At $p > 0.13$ mbar calcium vapour pressure may be accepted to be equal to $0.01\,p$. At $p < 0.13$ mbar, one may not neglect the above separation; it is impossible to estimate the calcium vapour pressure for this pressure range.

The technique under consideration allows one to vary the pressure of colouring metal vapour, calcium, from $\sim 6.7 \times 10^{-2}$ to $\sim 1.3 \times 10^{-3}$ mbar and to maintain it during the time sufficient for the homogeneous colouring of CaF_2 samples of considerable dimensions.

The CaF_2 colouring is executed at $T = 750$–850 °C. Heating time necessary to reach this temperature is around 2 h.

The heat-pipe dynamic mode provides implementation of about 100 colouring cycles using one portion of metal composition with good reproducibility of results including the low-pressure range, for which the exact value of calcium pressure cannot be estimated (see above).

When heated the crystal in the vapour–gas mixture used, calcium atoms are captured at the crystal surface, borrowing deficient fluorine ions out of the near-surface layers thus forming a new lattice layer. Anion vacancies created in near-surface layers and electrons, which arise due to reaction $Ca^0 \rightarrow Ca^{2+} + 2e^-$, diffuse into the crystal bulk due to sufficiently large vacancy mobility at the colouring temperature. Recombination of these components at the crystal cooling results in formation of various types of colour centres [30, 31].

The concentration of vacancies/electrons that can be introduced in CaF_2 crystals during the colouring depends on both temperature and calcium vapour pressure. Under stiff colouring conditions (relatively high T and p), this concentration reaches units of 10^{18} cm^{-3}.

In the colouring process, a relatively fuzzy border between coloured and non-coloured segments of the crystal (Fig. 2a) moves from the sample surfaces into its bulk until all volume of the sample appears uniformly coloured.

The colouring rate is mainly determined by the temperature. The homogeneous colouring of the $10 \times 10 \times 10$ mm sample of the crystal at $T = 830$ °C takes around 3.5 h.

Features of additive colouring of CaF_2 ceramics were studied in [35].

3 Features of the additive colouring of CaF_2:Yb crystals

3.1 Samples and results of their additive colouring

Unlike undoped CaF_2 crystals, when colouring crystals doped with RE ions, anion vacancies that diffuse into the crystal bulk recombine with interstitial F^- ions compensating the +1 extra-charge of RE^{3+} ions in as-grown crystal whereas electrons are captured by these ions thus converting them into a bivalent state.

CaF_2:Yb crystals used in this study were grown from high-purity initial material that had been additionally purified by melting together with PbF_2 scavenger with a concentration of 3 wt.%. Fluorinated dopant YbF_3 together with initial material and an additional quantity of PbF_2 scavenger were loaded into a Bridgmen-Stockbarger set-up with a multichannel crucible [36]. The crucible was a graphite cylinder of 130 mm diameter and 70 mm length with 24 growth channels of 16 mm diameter and 50 mm length each. Three of these channels were used for simultaneous growth of crystals with different Yb content; the channels were isolated from each other by a graphite shield plugs. The distribution coefficient of Yb in CaF_2 is close to unity [37, 38]. The homogeneous distribution of impurity over as-grown CaF_2:Yb crystals was observed in [25].

Three CaF_2:Yb crystals with Yb concentration of 2.2×10^{18}, 6.2×10^{18} and 1.1×10^{19} cm^{-3} as determined by a mass-spectrometric analysis were grown; samples fabricated from these crystals will be referred to as Sample 1, Sample 2 and Sample 3, respectively.

Absorption spectra of as-grown crystals recorded with a Cary-500 spectrophotometer are shown in Fig. 3. The band

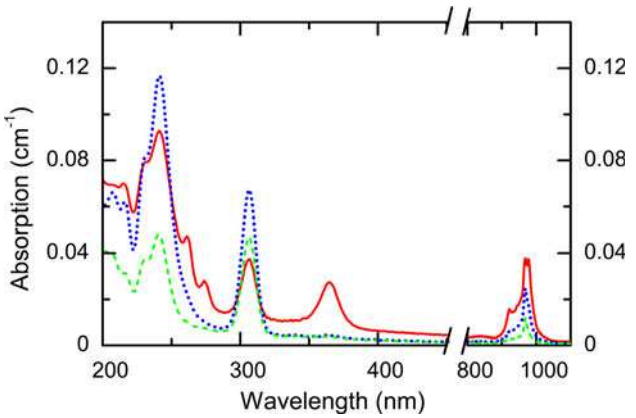

Fig. 3 Absorption spectra of as-grown: (*dashed line*) Sample 1, (*dotted line*) Sample 2, (*solid line*) Sample 3

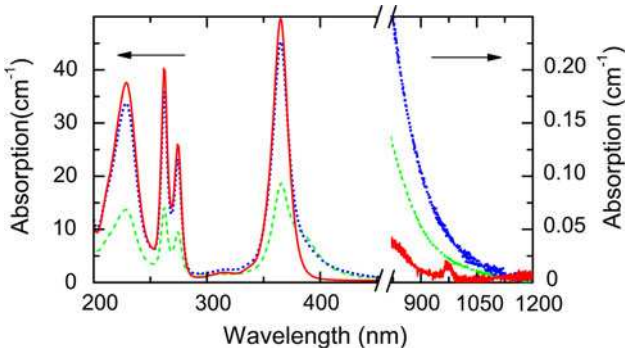

Fig. 4 Absorption spectra of additively coloured: (*dashed line*) Sample 1, (*dotted line*) Sample 2, (*solid line*) Sample 3

in the infrared (IR) range of the spectra is due to Yb^{3+} ions, whereas those in the UV range, together with Yb^{2+} bands 229.0. 262.2, 274.2 and 365.0 nm, contain several bands tied to $f \rightarrow d$ transition in trace RE^{3+} impurities, in particular, 306.0 nm band of Ce^{3+}. Note that relative intensities of Yb^{3+} and Yb^{2+} bands differ for various samples, which testifies to slightly differing reducing conditions in the growth process.

The rectangular samples $12 \times 12 \times 6$ mm for the additive colouring were cut out from these crystals. The colouring was executed at $T = 850$ °C and $p = 0.026$ mbar. In the same colouring conditions, two undoped CaF_2 samples $12 \times 12 \times 10$ mm were treated. One of these samples was homogeneously coloured for 2 h, whereas the second was coloured for 15 min to observe the border between coloured and non-coloured segments (Fig. 2a). The homogeneous colouring of Sample 1 and Sample 2 took 15 and 25 h, respectively; for both samples, the colouring was executed for several 5-h cycles (the time after reaching the working temperature). To observe the border between coloured and non-coloured segments, the Sample 2 was extracted from the set-up after the first two cycles and a photograph was taken through the 12×5 mm polished side facet (Fig. 2b). It was then returned into the set-up to continue the colouring procedure.

For Sample 3, the thickness of the coloured segment after 20 h colouration was about 1.5 mm. The homogeneous colouring of this sample was not performed since it needed too much time.

Unlike undoped crystals, the border between coloured and non-coloured segments of Yb-doped samples is extremely sharp (Fig. 2b).

Absorption spectra of additively coloured CaF_2:Yb samples are presented in Fig. 4.[2] One may see the disappearance of the Yb^{3+} band for Sample 1 and Sample 2. This means that a total $Yb^{3+} \rightarrow Yb^{2+}$ conversion took place for these samples. Correspondingly, the UV absorption of Yb^{2+} ions increased; bands of trace RE^{3+} ions disappeared. An $\sim$80 % decrease of intensity of the Yb^{3+} band is observed for the coloured segment of Sample 3. This means that $\sim 9 \times 10^{18}$ cm^{-3} vacancies were introduced into this sample in the process of its colouring. Using the method for determination of vacancy concentration for undoped CaF_2 crystals [31], we find that for the reference (undoped) sample, which was coloured in the same conditions, this concentration is 2×10^{17} cm^{-3}. Thus, the quantity of anion vacancies/electrons that can be introduced into CaF_2:Yb crystals with a Yb concentration of 1.1×10^{19} cm^{-3} exceeds by nearly two orders of magnitude the quantity for the undoped crystal.

3.2 Discussion of experimental results

The reason for the sharp slowing-down of additive colouring of Yb-doped samples is as follows. At the colouring temperature, together with the process of the capture of electrons by Yb^{3+} ions, the reverse process of thermal ionisation of Yb^{2+} ions is going on with the formation of free electrons. Frenkel defects, anion vacancies and interstitial F^- ions are formed simultaneously. Thus, a certain concentration of electrons and anion vacancies is maintained in the coloured region of the sample, where maximal possible (at given conditions) reduction of Yb ions occurred. As a result, the concentration gradient of these components between the coloured segment of the sample and its surface are reduced compared with undoped crystal. This diminishes diffusion fluxes of vacancies/electrons into the sample bulk, i.e. increases the colouring time. The larger the Yb concentration, the more is its colouration time.

The degree of diffuseness of a boundary between the coloured and non-coloured segments of the sample is determined by the diffusion path-length of the vacancy,

[2] Absorption spectrum of a thin ($\sim$1 mm) layer that was cut off the coloured segments of the crystal was recorded for Sample 3.

which is limited (in RE-doped crystals) by its recombination with interstitial F^- ions. A sharp boundary between coloured and non-coloured segments in RE-doped crystals indicates a threshold character of the dependence of a vacancy-free path on the reduction degree. Apparently, the threshold is reached when the concentration of compensating interstitial F^- ions becomes comparable to the concentration of "Frenkel" F^- ions. The achievement of this threshold limits the advance of vacancies into the uncoloured segment of the sample.

The flux of anion vacancies/electrons that diffuse into the sample bulk is determined by a difference in their concentration on the sample surface and in the adjacent (coloured) segment of the volume. The concentration in this segment depends on the production rate of these components. This rate in the coloured segment of undoped crystals is determined by the thermal dissociation of colour centres. The activation energy of this process is around 1 eV [39]. In crystals with high Yb content, electrons are mainly produced by the thermal ionisation of Yb^{2+} ions (activation energy $\sim$4 eV [40]). The main source of vacancies in these crystals is Frenkel pairs, whose formation energy is 2.7 eV [39]. Thus, the bulk generation of anion vacancies and electrons occurs more slowly in reduced segments of Yb-doped crystals than in such segments for undoped crystals with colour centres. This circumstance explains the much higher concentration of vacancies/electrons that can be introduced into Yb-doped crystals compared with undoped crystals.

One may see in Fig. 4, the decrease of IR absorption with increased wavelength for the coloured crystals (especially significant for Samples 1 and 2). The point is that at the crystal colouring, together with $Yb^{3+} \rightarrow Yb^{2+}$ conversion, a competitive process of colour centre formation takes place. The trifle quantity of these centres arises even during Yb^{3+} reduction; their formation continues after the total $Yb^{3+} \rightarrow Yb^{2+}$ conversion (Samples 1 and 2). The above-mentioned absorption decrease with wavelength increase is due to long-wavelength tails of near-IR bands of some centres (note also the highly stretched ordinate scale for the IR range in Fig. 4).

The same reason, i.e. the colour-centre formation, is responsible for the intensity increase at the long-wavelength wing of the 365.0 Yb^{2+} line for additively coloured Samples 1 and 2.

4 Determination of Yb^{2+} concentration in CaF_2:Yb crystals and ceramics

The concentration of Yb^{2+} ions in CaF_2:Yb crystal/ceramics can be determined provided that a cross section, σ, of a certain absorption line of this ion is known. The total $Yb^{3+} \rightarrow Yb^{2+}$ conversion in the Samples 1 and 2 allows determination of this quantity. The additively coloured Sample 2 was chosen for this purpose since its absorption spectrum is less disturbed by the colour centres than the spectrum of Sample 1 (Fig. 4). The cross section of the bands 365.0, 274.2 and 262.2 nm were determined by the formula

$$\sigma = k_2/N_2(\mathrm{Yb}), \quad (1)$$

where k_2 and N_2 (Yb) are the absorption coefficient of corresponding absorption band and Yb concentration in Sample 2, respectively. The found values of σ for these bands are given in the Table 1.

Table 1 Parameters of Yb^{2+} absorption spectrum of Sample 2

Absorption band (nm)	k (cm^{-1})	σ (10^{-18} cm^2)
365.0	45.85	7.40
274.2	23.70	3.82
262.2	36.32	5.86

Table 2 Yb^{2+} concentration in CaF_2 crystal/ceramics

Sample	N(Yb), 10^{20} cm^{-3}	k(365 nm), cm^{-1}	$N(Yb^{2+})$, 10^{17} cm^{-3}
Sample 4	7.82	1.33	1.80
Sample 5	6.52	0.22	0.30
Sample 6	6.52	0.13	0.18

The knowledge of these parameters enables estimation of $N(Yb^{2+})$ by the spectrum of any CaF_2:Yb crystal/ceramics by the formula:

$$N\left(Yb^{2+}\right) = k/\sigma, \quad (2)$$

where k is the absorption coefficient of one of these bands in the spectrum of the sample under study and σ is the cross section of this line.

To illustrate the application of this technique, the spectra of three samples with typical "laser" concentrations of Yb were recorded (Table 2): (1) as-grown CaF_2:Yb crystal (Sample 4, Fig. 5); (2) as-fabricated CaF_2:Yb ceramics (Sample 5, Fig. 6); (3) the same ceramics subjected to fluorination (Sample 6, Fig. 6). The spectra of these samples show a non-structured background; it is significantly more expressed in ceramics than in crystals with similar Yb^{2+} concentration. As seen in Fig. 6, the background is partly tied to the Yb^{2+} content; however, their causal connection is not clear.

The approximation of background for the spectral range $\sim$250–400 nm, in which the above-mentioned bands are found, needs the use of high-order polynomial function; for Sample 5, such an approximation is problematic. Therefore, the band 365 nm relatively isolated in the spectrum was chosen for estimation of the Yb^{2+} concentration. We propose that for the referent Sample 2 $k(330\ \mathrm{nm}) = k(400\ \mathrm{nm}) \approx 0$

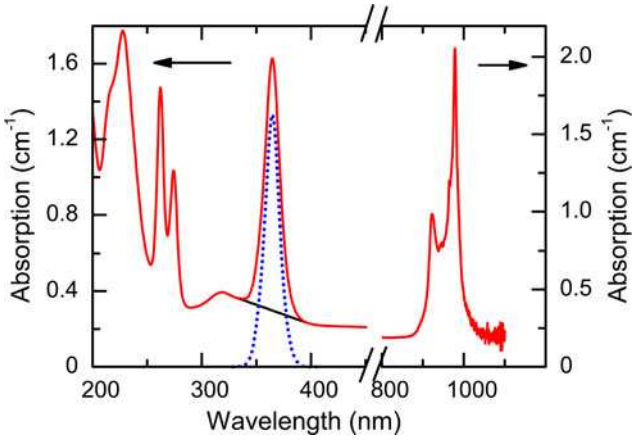

Fig. 5 Absorption spectrum of as-grown CaF_2:Yb crystal (Sample 4). The *straight line* shows the background approximation. *Dotted line* shows the 365 nm band after background correction

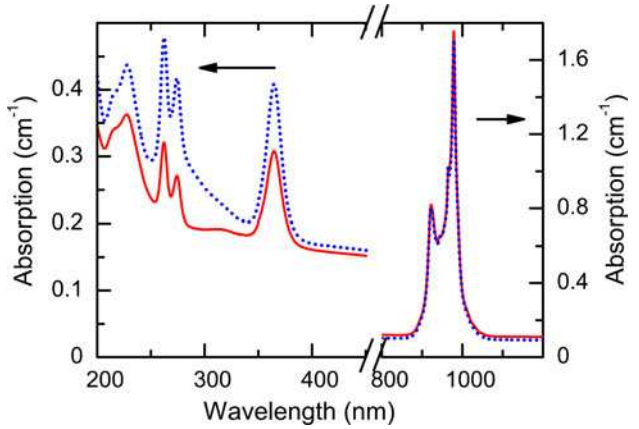

Fig. 6 Absorption spectra of: (*dotted line*) as-fabricated optical ceramics (Sample 5) and (*solid line*) the same ceramics after the fluorination procedure (Sample 6)

and approximated the background for Samples 4–6 in the spectral range 330–400 nm by a straight line. The subtraction of its ordinates out of k meanings gives an approximate shape of 365 nm band "purified" from the background. This procedure is shown for Sample 4 in Fig. 5. The background approximation by the second-order polynomial function gives practically the same band shape.

The σ (365.0) parameter and k peak meanings for the purified bands were used to estimate the values of $N(Yb^{2+})$ for samples under study accordingly to Eq. (2). These values are given in Table 2 together with the total Yb concentrations in the samples.

5 Conclusions

An additive colouring technique has been used for the total conversion of Yb^{3+} ions in low-concentration CaF_2:Yb crystals into a bivalent state. Significant distinctions in the colouring of undoped and RE-doped crystals have been found. The colouring of RE-doped crystals is occurring much slower than compared to undoped crystals, the border between coloured and non-coloured segments of the samples is considerably more distinctive, and the concentration of anion vacancies/electrons introduced into the samples at its colouring is much higher. The physical mechanisms responsible for these distinctions are discussed. It was found that for crystals with Yb concentration that do not exceed $\sim 6 \times 10^{18}$ cm^{-3}, the colouring conditions used in this study ensure the total conversion of Yb^{3+} ions present in the crystal into a bivalent state. This fact made it possible to find the cross-sections of several Yb^{2+} absorption bands. The knowledge of these parameters allowed estimation of the Yb^{2+} content in as-grown CaF_2:Yb crystal and two samples of CaF_2:Yb ceramics, as-fabricated and fluorinated after the fabrication.

References

1. W.F. Krupke, IEEE J. Sel. Top. Quant. **6**, 1287 (2000)
2. V. Petit, J.L. Doualan, P. Camy, V. Ménard, R. Moncorgé, Appl. Phys. B **78**, 681 (2004)
3. A. Lucca, M. Jacquemet, F. Druon, F. Balembois, P. Georges, P. Camy, J.L. Doualan, R. Moncorgé, Opt. Lett. **29**, 1879 (2004)
4. A. Lucca, G. Debourg, M. Jacquemet, F. Druon, F. Balembois, P. Georges, P. Camy, J.L. Doualan, R. Moncorgé, Opt. Lett. **29**, 2767 (2004)
5. M. Siebold, M. Hornung, R. Boedefelt, S. Podleska, S. Klingebiel, C. Wandt, F. Krausz, S. Karsch, R. Uecker, A. Jochmann, J. Hein, M.C. Kaluza, Opt. Lett. **33**, 2770 (2008)
6. M. Siebold, S. Bock, U. Schramm, B. Xu, J.L. Doualan, P. Camy, R. Moncorgé, Appl. Phys. B **97**, 327 (2009)
7. J.L. Doualan, P. Camy, A. Benayad, V. Ménard, R. Moncorgé, J. Boudeile, F. Druon, F. Balembois, P. Georges, Laser Phys. **20**, 533 (2010)
8. G.A. Slack, Phys. Rev. **122**, 1451 (1961)
9. J. Boudeile, J. Didierjean, P. Camy, J.L. Doualan, A. Benayad, V. Ménard, R. Moncorgé, F. Druon, F. Balembois, P. Georges, Opt. Express **16**, 10098 (2008)
10. P.A. Popov, P.P. Fedorov, S.V. Kuznetsov, V.A. Konyushkin, V.V. Osiko, T.T. Basiev, Dokl. Phys. **53**, 198 (2008)
11. P.A. Popov, P.P. Fedorov, V.A. Konyushkin, A.N. Nakladov, S.V. Kuznetsov, V.V. Osiko, T.T. Basiev, Dokl. Phys. **53**, 413 (2008)
12. S.A. Kazanskii, Sov. Phys. JETP-USSR **57**, 1202 (1983)
13. C.R.A. Catlow, A.V. Chadwick, G.N. Greaves, L.M. Moroney, Nature **312**, 601 (1984)
14. D.J.M. Bevan, S.E. Ness, M.R. Taylor, Eur. J. Sol. State Inorg. Chem. **25**, 527 (1988)
15. S.A. Kazanskii, A.I. Ryskin, Phys. Solid State **44**, 1415 (2002)
16. S.A. Kazanskii, A.I. Ryskin, A.E. Nikiforov, A.Yu. Zakharov, M.Yu. Ougrumov, G.S. Shakurov, Phys. Rev. B **72**, 014127 (2005)
17. V. Petit, P. Camy, J.-L. Doualan, X. Portier, R. Moncorgé, Phys. Rev. B **78**, 085131 (2008)
18. F. Druon, S. Ricaud, D.N. Papadopoulos, A. Pellegrina, P. Camy, J.-L. Doualan, R. Moncorgé, A. Courjaud, E. Mottay, P. Georges, Opt. Mater. Express **1**, 489 (2011)

19. P.P. Fedorov, V.V. Osiko, T.T. Basiev, Yu. V. Orlovskii, K.V. Dykel'skii, I.A. Mironov, V.A. Demidenko, and A.N. Smirnov, *Optical Fluoride and Oxysulphide Ceramics: Preparation and Characterization.* In: *Developments in Ceramic Materials Research* (NOVA Science Pub., Inc., New York, 2007)
20. T.T. Basiev, M.E. Doroshenko, P.P. Fedorov, V.A. Konyushkin, S.V. Kuznetsov, V.V. Osiko, M.Sh. Akchurin, Opt. Lett. **33**, 521 (2008)
21. A. Lyberis, G. Patriarche, P. Gredin, D. Vivien, M. Mortier, J. Eur. Ceram. Soc. **31**, 1619 (2011)
22. P.P. Fedorov, V.V. Osiko, S.V. Kuznetsov, E.A. Garibin, J. Phys: Conf. Ser. **345**, 012017 (2012)
23. M.Sh. Akchurin, T.T. Basiev, A.A. Demidenko, M.E. Doroshenko, P.P. Fedorov, E.A. Garibin, P.E. Gusev, S.V. Kuznetsov, M.A. Krutov, I.A. Mironov, V.V. Osiko, P.A. Popov, Opt. Mater. **35**, 444 (2013)
24. S.M. Kaczmarek, T. Tsuboi, M. Ito, G. Boulon, G. Leniec, J Phys-Condens Mat **17**, 3771 (2005)
25. I. Nicoara, N. Pecingina-Garjoaba, O. Bunoiu, J. Cryst. Growth **310**, 1476 (2008)
26. A. Smakula, Phys. Rev. **77**, 408 (1950)
27. V.A. Arkhangelskaya, M.N. Kiseleva, Fiz. Tverd. Tela **9**, 3523 (1967) (in Russian)
28. F.K. Fong, J. Chem. Phys. **41**, 2291 (1964)
29. Z.J. Kiss, P.N. Yocom, J. Chem. Phys. **41**, 1511 (1964)
30. A.S. Shcheulin, T.S. Semenova, L.F. Koryakina, M.A. Petrova, A.K. Kupchikov, A.I. Ryskin, Opt. Spectrosc. **103**, 660 (2007)
31. A.S. Shcheulin, T.S. Semenova, L.F. Koryakina, M.A. Petrova, A.E. Angervaks, A.I. Ryskin, Opt. Spectrosc. **110**, 617 (2011)
32. C.Z. van Doorn, Philips Res. Reports. Suppl. **4**, 1 (1962)
33. R.C. Alig, Z.J. Kiss, J.P. Brown, D.S. McClure, Phys. Rev. **186**, 276 (1969)
34. G.J. Pogatshnik, D.S. Hamilton, Phys. Rev. B. **36**, 8251 (1987)
35. A.S. Shcheulin, A.I. Ryskin, A.E. Angervaks, P.P. Fedorov, V.V. Osiko, A.A. Demidenko, E.A. Garibin, A.N. Smirnov, K.V. Dukel'skii, I.A. Mironov, Opt. Spectrosc. **110**, 604 (2011)
36. I. Nicoara, L. Lighezan, M. Enculescu, I. Enculescu, J. Cryst. Growth **310**, 2026 (2008)
37. V.V. Karelin, M.Z. Kazakevich, A.F. Redkin, V.E. Bozhevolnov, G.V. Molev, V.I. Korobkov, B.P. Sobolev, Sov. Phys. Crystallogr. **20**, 464 (1975)
38. F. Delbove, S. Lallemand-Chatain, CR Acad. Sci. C. Chim. **270**, 964 (1970)
39. W. Hayes (ed.), *Crystals with the Fluorite Structure: Electronic, Vibrational, and Defect Properties* (Clarendon Press, Oxford, 1974)
40. V.A. Arkhangelskaya, M.N. Kiseleva, V.M. Shraiber, Fiz. Tverd. Tela **11,** 870 (1969) (in Russian)